3D printing and milling accuracy influence on full-contour zirconia crown adaptation

Bernardo Camargo[1], Evita Willems[1,2], Wout Jacobs[1], Kirsten Van Landuyt[1], Marleen Peumans[1], Fei Zhang[1,2], Jef Vleugels[2], Bart Van Meerbeek[1]

[1]KU Leuven, Department of Oral Health Sciences, BIOMAT - Biomaterials Research Group & UZ Leuven (University Hospitals Leuven), Dentistry, Kapucijnenvoer 7 blok a, B-3000 Leuven, Belgium; [2]KU Leuven, Department of Materials Engineering, Kasteelpark Arenberg 44, B-3001 Leuven, Belgium.

Corresponding author:

Prof. Dr. Bart VAN MEERBEEK
Department of Oral Health Sciences (OHS)
Biomaterials Research group - BIOMAT
Kapucijnenvoer 7 blok a - bus 7001
3000 Leuven - Belgium
bart.vanmeerbeek@kuleuven.be

3D printing and milling accuracy influence full-contour zirconia crown adaptation

Bernardo Camargo[1], Evita Willems[1,2], Wout Jacobs[1], Kirsten Van Landuyt[1], Marleen Peumans[1], Jef Vleugels[2], Bart Van Meerbeek[1]

[1]KU Leuven, Department of Oral Health Sciences, BIOMAT - Biomaterials Research Group & UZ Leuven (University Hospitals Leuven), Dentistry, Kapucijnenvoer 7 blok a, B-3000 Leuven, Belgium; [2]KU Leuven, Department of Materials Engineering, Kasteelpark Arenberg 44, B-3001 Leuven, Belgium.

ABSTRACT

Objectives: To correlate trueness and cement-space characteristics of crowns milled chairside and in the laboratory with those of inkjet 3D-printed crowns, and to assess whether 3D-printing accuracy meets the clinical standard.

Methods: Thirty crowns were either (1) milled using a chairside Cerec MCXL unit from Cerec Zirconia Mono L (Dentsply Sirona), (2) milled using a LX-O 5-axis (Matsuura Machinery) industrial machine from Initial Zirconia HT (GC), or (3) 3D-printed using an inkjet Carmel 1400C (Xjet) printer (n=10). Crown trueness determined by comparing the original CAD with each visible-light digitized crown was correlated with the 3D cement-space characteristics recorded by micro-CT. Statistics involved Kruskal-Wallis testing and Spearman correlation.

Results: Crown trueness at the intaglio marginal area positively correlated with the marginal and axial cement-space characteristics. 3D-printing revealed data in-between those of the two milling systems with undercut values being not statistically different from those recorded for chairside milling and a low overcut level that was statistically similar to that obtained by laboratory milling. Laboratory milling revealed a significantly better marginal accuracy with a consequently lower cement-space thickness. A higher overcut level was recorded for the chairside-milled crowns in the

marginal/occlusal thirds, resulting in the significantly highest occlusal cement-space thickness and cement-volume percentage with a cement thickness above 120 µm (limit considered as clinically acceptable). No statistical difference in trueness was found for the external crown dimensions.

Significance: The 3D-printed zirconia crowns provided sufficient manufacturing accuracy for clinical use. Accurate milling and printing of the crown's intaglio marginal area is primordial.

INTRODUCTION

Fixed dental prosthesis (FDP) manufacturing has evolved over the last decades, shifting from conventional techniques to computer-aided design and manufacturing (CAD/CAM) [1]. As alternative for the well-established milling or substractive manufacturing (SM), additive manufacturing (AM) or 3D-printing is currently emerging, aiming for more individualized (multi-shade/translucency, multi-material) restorations, as well as fabrication efficiency, standardization, and accuracy [2–4]. Even so FDP manufacturing today involves more digital processing, caries and loss of retention are still the two most common reasons of FDP failure, both associated with suboptimal restoration-prep adaptation [5]. To achieve optimum adaptation, the manufacturing process is an essential step, with superior trueness in the CAM process facilitating a better fit [6]. However, trueness values provided in literature are difficult to interpret and in particular their immediate clinical relevance associated with the restoration adaptation is not always clear [7].

Along with the evolution in the manufacturing process, all-ceramic crowns have been developed and high-strength ceramics such as zirconia have been introduced. Thanks to the natural aesthetics and mainly to the highest fracture toughness and flexural strength of any dental ceramic [8], the use of zirconia restorations has boomed in recent years [1]. Currently, different dental zirconia grades can be distinguished, this based on yttria content with different strengths and translucencies: the strongest and opaque 3 mol% yttria-stabilized tetragonal zirconia polycrystalline (3Y-TZP), the more translucent but slightly weaker 4 mol% yttria partially stabilized zirconia (4Y-PSZ), and the most translucent but mechanically weakest 5 and 6 mol% 5Y/6Y-PSZ. In addition, multi-layered shade-

gradient (3Y-TZP, 4Y or 5Y-PSZ) and strength-gradient (3Y-TZP cervical combined with 4Y- or 5Y-PSZ incisal/occlusal) zirconia ceramics are marketed [9,10]. However, the fabrication process of zirconia restorations is very critical. To achieve maximum strength and density, zirconia is sintered, which is accompanied with 15-30% shrinkage in volume. Hence, zirconia restorations have to be designed and milled oversized to compensate for the subsequent sintering shrinkage, upon which the final restoration dimensions are reached [11]. This process could distort the original restoration design (CAD). The zirconia FDP adaptation hence depends on two production variables: the device's accuracy to fabricate the restoration and the 3D-control of the sintering shrinkage [3]. The highest milling accuracy is yielded by five-axis milling devices in dental milling centers and laboratories [12]. A faster and more simplified production way is chairside milling, with the well-established Cerec (Dentsply Sirona, Bensheim, Germany) CAD/CAM system constituting a reliable and efficient chairside alternative frequently used in dental practices [6]. However, the less favorable crown fit resulting from chairside CAD/CAM keeps its accuracy being regarded in literature as questionable [2,13,14]. Furthermore, SM has inherent limitations, such as considerable waste of material when the restoration is cut out of a block/disk, the device's axis number to mill, the size/coarseness of the milling burs, the constant need to replace milling tools after a number of cycles, the reproduction limitations regarding surface geometry as dictated by the size of the milling burs and axis of the machine, and the continuously existing risk of introducing micro-cracks [4].

AM is a minimum waste manufacturing process that could overcome many of the above-described deficiencies of SM, while further optimization of current AM technology for dental restorations remains definitely needed.

Essential is to be aware of the accuracy of manufacturing, its random and systematic errors, as well as the limitations that could affect the designed and produced restoration [7]. Numerous processing factors, among which the machining mechanical loads, vibrations, shocks, the tool wear and geometry, as well as the sintering and de-binding process can negatively affect the FDP's adaptation to the prep, ultimately compromising the restoration's clinical lifetime [7,15,16]. It is known that better manufacturing accuracy, measured as trueness, will result in a better FDP fit [17]. However,

most studies in literature either focused solely on measuring trueness or on measuring its consequence, i.e. the final crown adaptation. The latter is assessed mainly by measuring marginal discrepancies. Although at present there is no industrial standard for assessing trueness of dental restorations, a last-generation 3D visible-light scanner can guarantee consistent trueness data. This method uses a 3D scanner to recreate the object's geometrical shape by collecting distance information from different object-surface points. In a further step, trueness is measured by calculating the degree of deviation between the scanned 3D model of the manufactured crown in relation to the original CAD [6].

No standard protocols exist to measure an FDP's fit, while also a clear definition of an adequate crown adaptation has yet to be defined [4,18]. Due to methodological limitations but also author preferences, to date there is no single definition of what can be considered as a 'clinically acceptable' cement space [19,20]. Conventional methodologies usually involve microscopy following destructive specimen-preparation methods. Gaps sizes are two-dimensionally estimated at randomly selected sections, hereby strongly depending on the cross-sectioning angle [4,21,22]. Several methodological critiques were reported in the literature, such as difficulties to repeat measurements from an identical angle, intrinsic inaccuracies associated with the impression and duplication of each model, and the limited number of measurement points used to reveal consistent and clinically relevant data [3,4,20,23]. Another critical issue is to combine considerable variations in gap size, measured horizontally and vertically, into one mean gap size. Although a mean gap size may well be within a clinically acceptable range, defects such as chipping or premature contacts interfering with complete FDP seating, will be masked, barely detected and measured [19,22]. Consequently, most authors agree that conclusions based on a mean marginal gap-size value do not provide adequate information on the clinical acceptability of a restoration's fit [19,24]. A full 3D description of the relationship between FDP and tooth prep (e.g. cement space) very likely provides more clinically meaningful information and has been addressed by the introduction of a 3D non-destructive fully quantitative approach using micro-computed tomography (micro-CT) [18]. With this methodology, the pre-cementation cement-space volume and thickness can be quantified in a huge number of

virtual sections. It also enables to fit each fabricated crown on one and the same master model, not requiring any model reproduction. Finally, no cement-space volume and thickness data are lost, which is the case when a specimen-destructive sectioning methodology is employed [18,19,25].

Accurate FDP adaptation and long-term marginal stability are intimately connected with the cement-space characteristics [26]. Even though no consensus exists in literature what the 'ideal' cement-space thickness is [27,28], a cement space as uniform and thin as possible is desired, since a non-uniform and thick cement layer has been associated with earlier failure [29,30]. Furthermore, in a more comprehensive view, the mechanical stability and overall clinical performance are differently affected by the specific cement-space characteristics in the marginal, axial and occlusal thirds [22,31]. Inadequate marginal adaptation with increased cement exposure is associated with enhanced (micro/nano-)leakage and biological risks, such as plaque retention, causing gingival inflammation and secondary caries in the long term [1]. Besides biological aspects, the marginal area has been shown to contribute to crown retention, which is defined as a dental prosthesis' quality to resist dislodgment forces. Along with their taper and convergence angle, the axial walls also influence restoration retention, with a wide gap size at the axial third resulting in lower retention [32]. Additionally, an increased cement space in the occlusal third decreases the fracture strength of the restored tooth due to different load concentrations and force dissipations, increasing stress build-up during functioning (chewing) [22]. Hence, full 3D characterization of marginal adaptation and the whole cement space provides information of high clinical relevance with regard to an FDP's expected lifetime.

Although crown trueness is in theory closely related to crown adaptation [33], to the best of our knowledge, no published studies have explored this relationship and none have combined visible-light scanning and micro-CT as two high-tech methodologies to assess this relationship. With an innovative approach merging visible-light scanning and micro-CT, an in-depth study of the influence of zirconia FDP trueness on the cement-space characteristics was conducted non-destructively in 3D. Since limited information is available regarding 3D-printed zirconia crowns and no data at all regarding crowns printed by inkjet technology [34,35], the geometric accuracy of 3D-printed zirconia FDPs

remains unclear [36]. This study compared a 3D-printing manufacturing process of zirconia FDPs with chairside and laboratory milling manufacturing. Both the crown intaglio's surface area and the pre-cementation gap were virtually divided into marginal, axial, and occlusal areas/thirds. Each area's trueness was evaluated, and the results were associated with the corresponding volume and thickness of the cement space. The first research question to be answered was if the trueness of one of the three intaglio surface areas has a higher influence on the crown adaptation. The first null hypothesis tested was that there was no difference in influence of the three intaglio surface areas on the crown adaptation (or fit). The second research question addressed was to investigate if inkjet 3D-printing is accurate enough to fabricate FDPs for clinical use. The second null hypothesis tested was that there was no difference in geometric accuracy and subsequent crown adaptation among the 3D-printed crowns as compared to the chairside and laboratory milled crowns.

MATERIALS AND METHODS

Tooth preparation and crown manufacturing

An extracted human caries-free maxillary molar (approved by the Commission for Medical Ethics of KU Leuven under the file number S64350) was manually prepared for a full crown. Using a new coarse (151 µm) parallel chamfer diamond bur (8881, Komet, Lemgo, Germany) in a high-speed air turbine, the occlusal surface was reduced with 2 mm, resulting in a shallow concavity prepared at the tooth center between the reduced buccal and palatal cusps. The axial walls were next prepared with a new coarse (151 µm) tapered chamfer diamond bur with guide pin (6856P size 021, Komet) in a red-banded counter-angle rotary instrument under thorough water cooling to reach via the guide pin a cutting depth of 0.54 mm at the cervical crown-prep margin. All internal prep-transition angles were rounded off except for the crown-prep margin which was kept sharp.

An optical impression of the tooth prep was next made using a CEREC Omnicam camera (CEREC AC Omnicam, Dentsply Sirona). Using the Cerec SW 4.6 (Dentsply Sirona) software, the crown margin was marked manually to define the preparation-finish line, upon which the crown was designed

using the Cerec 'Biogeneric individual' software tool to achieve the 'master' CAD model. In the software's restoration parameters, the minimum ceramic thickness was set to 1.5 mm and the spacer thickness at 80 µm, this following the Cerec parameter guidelines for milling Cerec Zirconia restorations (Dentsply Sirona). After the design, the master CAD crown was saved in a standard .stl file format and exported to the three manufacturing devices, coded as 'Cerec_zir', 'Ini_HT' and 'XJet' (see below) as based on the material/device used. In total, 30 crowns (n=10) were manufactured, as follows:

Cerec_Zir: In the chairside milling SM group, the designed crown was milled from 10 pre-sintered CEREC Zirconia (CEREC Zirconia, Dentsply Sirona) blocks using a chairside CEREC MCXL (Dentsply Sirona) milling device in the 'fine' milling mode. Residual milling dust was removed from the pre-sintered restoration surface, first with pressurized air and then with a large sable brush (Isabey Pinceaux, Saint-Brieuc, France; size 10). The 10 crowns were next sintered individually in a CEREC SpeedFire (Dentsply Sirona) oven, with the restoration's occlusal surface facing downwards without supporting structure. The restoration was removed from the oven using tweezers and placed for 2 min on the CEREC SpeedFire's fan area until cool to the touch.

Ini_HT: In the laboratory milling SM group, 10 crowns were milled out of pre-sintered Initial High Translucency (HT) (GC, Tokyo, Japan) zirconia disks using a Matsuura LX-O 5 axis (Matsuura Machinery, Leicestershire, England) industrial milling machine. Residual milling dust was removed with pressurized air and a large sable brush (Isabey Pinceaux), as described above. The crowns were next sintered using a Dekema Austromat (Dental-Keramikofen, Freilassing, Germany) oven using the manufacturer's recommended parameters (1450°C for 6h and 30min with a heating and cooling rate of 8,4°C/min).

XJet: A commercial Carmel 1400 (Xjet) inkjet printer was used. Willems *et al.* [36] conducted a comprehensive study of the microstructure and mechanical properties of 3D-printed 3Y-TZP ceramics fabricated by inkjet printing. In summary, the inkjet process consists of the deposition of the ZrO_2-ceramic ink surrounded by an envelope of support material with a programmed resolution of 16.000 x 17.625 µm and a layer thickness of 10.5 µm. The ceramic part was built by small droplets of a

commercial ZrO_2 suspension (C800 zirconia model dispersion grade 7250001, XJET), which contains about 45wt% ZrO_2 powder in a proprietary mixture of glycol ethers and dispersing agent. The envelope consisted of pillars made of ZrO_2-ink filled with support ink (SC300, XJET) that consists of 31wt% sodium carbonate in a mixture of glycol ether and dispersing agent. Upon deposition of each layer, a heating lamp together with a base plate heated at 180°C moved over the printed layers to evaporate the printed ink's solvent, immediately followed by an integrated metal roller that passed over the dried printing bed, trimming the surface to achieve the desired height. The printed crown was separated from the pillar envelope by a space of 300 µm, enabling easy removal of the envelope during post-printing washing. Washing is done by submerging the printed crown in demineralized water for 6-8 hours to remove the support structures and detach the parts from the building platform by disintegrating the support ink material. The washed and removed prints were next placed on a metal raster to allow uniform drying in ambient air overnight. The obtained printed parts (green bodies) were subsequently de-binded in a muffle furnace (laboratory furnace RHF 1200, Carbolite, Hope Valley, UK) at a heating rate of 0.7°C/min up to 600°C with a 1-h dwell time, followed by sintering in air at 1450°C for 2 h with a heating and cooling rate of 5°C/min in a high-temperature furnace (Chamber Furnace HT 16/17, Nabertherm, Lilienthal, Germany) [36]. The crowns were printed with the inner surface faced up, showing a high green density of 57.7±0.3 g/cm^3 [36].

All three chosen zirconia are 3 mol% Y_2O_3-stabilized ZrO_2 (3Y-TZP). The sintered crown density was 6.07±0.1 g/cm^3, 6.06±0.1 g/cm^3 and 6.02±0.1 g/cm^3 for Cerec_Zir, Ini_HT, and XJet, respectively. No additional processing, such as finishing and polishing, was performed.

Visible-light scanning

Each crown was scanned using the industrial visible-light GOM compact 5M (GOM branch Benelux, Leuven, Belgium) non-contact scanner with a scanning resolution of 12 megapixels, by which individual .stl files were generated. The virtual model (.stl) generated by each crown scanning was checked in terms of minimal thickness using 3-Matic (Materialise, Leuven, Belgium) software. Using the same software, these virtual crowns were superimposed on the reference CAD file with a best-fit

alignment for every surface point (±40.000 points). Then, each scanned crown was subjected to a point-by-point surface comparison with the original CAD design. The International Organization for Standardization (ISO) describes 'accuracy' as the closeness of agreement between a measured value and a true value of a measured object (ISO/IEC GUIDE 99:2007 (E/F)). A high accuracy system can produce an object that is closely comparable to the CAD file [37]. Per definition, 'accuracy' involves two parameters: 'precision', which delivers information about the closeness of repeated measurements, and 'trueness', which provides information about the deviation from the true value [38]. TRUENESS was expressed in this study in 'overcut' (minimum: min) and 'undercut' (maximum: max) deviations, and 'trueness deviation' (root mean square: RMS), the latter indicating the deviation from zero between the two different datasets, disregarding whether it was located over or under the reference surface. Overcut (min) represents inaccuracies at regions where too much material was cut (or was chipped off) or not printed, with higher min values indicating more severe overcuts. Undercut (max) represents inaccuracies at regions where material was not sufficiently cut or too much printed, hereby potentially resulting in contacts that may hinder a correct fit; higher max values indicate more severe undercuts. Low trueness deviation (RMS) indicates a high degree of 3D matching and thus a high 3D trueness [33,39,40].

For an in-depth analysis of trueness in terms of 'overcut', 'undercut' and 'trueness deviation', distinction was made between the 'intaglio' (internal) surface AREAS and the 'external' surface area (area in mm^2). The intaglio surface area was further subdivided into 'marginal', 'axial', and 'occlusal' areas (Fig. 1a,b), as being defined as follows (Wang *et al*. [39]): 'intaglio marginal area' as ranging from the bottom marginal limit to 1 mm above, 'intaglio occlusal area' as ranging from the top occlusal surface to 1 mm below, and 'intaglio axial area' as ranging between the boundaries of the intaglio marginal and occlusal areas. Color maps were generated to represent 'trueness deviation' as shown in Fig. 1c; the boundary values were set at -120 µm and +120 µm.

Micro-computed tomography (micro-CT)

The cement space was imaged in 3D using X-ray micro-CT (Phoenix NanoTom, GE, Wunstorf, Germany) with a pixel size of 6.4 µm, 150 kV, 180 µA, and a 1-mm-thick copper filter (Fig. 1d). The acquisition was done with the crown-tooth set in the same position, over 360 degrees, leading to an average scanning time of approximately 40 min. The crowns were positioned on the master prep without cementation to avoid that the cement would affect the crown fit/adaptation [41,42]. Therefore, each crown was held in position on the tooth prep using a tiny drop of melted soft wax (Inlay Wax Soft, GC), which was added by the operator wearing magnifying loupes onto the occlusal prep surface using an SJK Dental Lab Electric Wax Knife (SJK Dental: www.sjkdent.com, China) with a fine tip (similar to a dental probe). Shortly after, the crown was seated with finger pressure until complete adaptation/seating was achieved. Similar as done during clinics, a fine dental probe was used to check the marginal adaptation/seating. The crown-prep assembly was next carefully wrapped using laboratory wrapping film (Parafilm M, Bemis, Neenah, WI, USA) to also externally hold the crown in place on the prep. The wrapped assembly was then attached onto the micro-CT holder.

The 3D cement-space volume was next virtually divided into three THIRDS: 'occlusal', 'axial' and 'marginal' thirds, this following the same guidelines as being defined above [25] (Fig. 1a,b). The parameters 'cement-space volume', 'cement-space thickness' and the 'cement-space volume distribution over thickness' (Fig. 1e), as proposed by Santos *et al.* (2020), were used to compare the CROWN ADAPTATION of the three manufacturing processes [25]. Cement-space thickness was defined as the diameter of the largest sphere, hereby fulfilling two conditions: (1) the sphere enclosed at least one voxel, which not necessarily was the center of the sphere; (2) the sphere was entirely bounded within the cement gap [43]. A cement-space thickness below 120 µm was considered as 'clinically acceptable', as was proposed by McLean and von Fraunhofer [44] and approximately corresponds to the dimension of a dental probe tip [7]. The 'clinically acceptable' (<120 µm) cement-space thickness percentage was recorded for each crown-prep set.

Scanning Electron Microscopy (SEM)

Based on the above findings, a total of 12 crowns (n=4 per device) were processed. The samples were placed in the center of an aluminum cylinder to which beforehand conductive carbon tape was attached. Conductive varnish (Leit-C, Sigma-Aldrich, Hoeilaart, Belgium) was used to enhance conductivity before gold-sputtering the specimens under a vacuum of 5mA/Pa (JFC-1300, JEOL, Tokyo, Japan). The specimens were then examined by SEM (JSM-6610LV, JEOL) .

Statistical analysis

Statistical analysis was conducted using SPSS (SPSS v22, IBM, Armonk, NY, USA), with statistical significance assessed using non-parametric Kruskal-Wallis test (α=0.05) with Bonferroni correction for multiple tests. Correlation between trueness and cement-space characteristics was evaluated using the Spearman correlation test.

RESULTS

Regarding TRUENESS (Table 1 and Fig. 2a-c), significantly higher trueness (values closer to zero) was recorded in terms of undercut (max) and trueness deviation (RMS) for Ini_HT for the intaglio marginal area (Table 1; Fig. 2a-c). Significantly higher overcut (min) was recorded for Cerec_Zir as compared to the other two groups for the intaglio occlusal area (Table 1/Fig. 2a-c).

Regarding CROWN ADAPTATION analyzed using micro-CT (Table 2 and Fig. 2d-f), the overall significantly best crown adaptation in terms of 'cement-space volume' and 'cement-space thickness', as well as 'cement-space percentage with a thickness below 120 µm', considered as norm of a 'clinical acceptable' cement-space thickness, was recorded for Ini_HT. From the whole Ini_HT crown-adaptation volume, 73% was considered clinically acceptable (<120 µm). Clinically acceptable cement-space thickness percentages above 90% were recorded for Ini-HT at the marginal and axial thirds. In 11 out of the 12 crown-adaptation measurements, Cerec_Zir significantly underperformed for crown adaptation as compared to Ini-HT. With 55%, the significantly lowest clinically acceptable

cement-space percentage (<120 µm) was recorded for Cerec_Zir (whole crown adaptation), with 79% and 64% being recorded at the marginal and axial thirds. Xjet scored in between Ini_HT and Cerec_Zir, reaching clinically acceptable cement-space thickness percentages of 65%, 89% and 73%, respectively, for the whole crown-adaptation volume, and at the marginal and axial thirds. Xjet significantly underperformed Ini_HT in 7 of the 12 crown-adaptation measurements, while significantly outperformed Cerec-Zir in 4 of the 12 crown-adaptation measurements. For all three experimental groups, the crown adaptation was worst at the occlusal third. Plotting the cement-space volume distributed by cement-space thickness revealed the lowest, the most left-shifted and most uniform cement space for Ini-HT at the marginal third, with the cement-space curves being very similar for Cerec_Zir and Xjet (Fig. 3). At the axial third, the highest clinically acceptable cement space (<120 µm) was recorded for Ini-HT. The lowest clinically acceptable cement space (<120 µm) was recorded at the occlusal third for all three experimental groups.

"SPEARMAN CORRELATION revealed significant correlation between trueness of the marginal area and the whole crown adaptation, mainly in the axial third. No correlation was found in the occlusal third with regard to both trueness and cement-space characteristics (Table 3)."

SCANNING ELECTRON MICROSCOPY (SEM) revealed specific manufacturing characteristics, such as the bur-sweeping direction separated by discretization steps (milling lines) for laboratory (Fig. 5a) and chairside milling (Fig. 5b). The characteristic 3D-printing surface-stepping phenomenon, resulting in a superficial line texture, was not clearly observed, most likely due to the sintering process following the 3D printing (Fig. 5c). Manufacturing flaws were also qualitatively examined, such as support-material agglomerates (Fig. 4a) as well as chipping defects at restoration margins in SM processing (Fig. 4d).

DISCUSSION

This study showed that there is a statistically relevant correlation between trueness of the marginal area and the whole crown adaptation. Consequently, a mismatch in the marginal area can lead to a

cascade effect that may also influence the crown adaptation at the axial and occlusal thirds, regardless of the manufacturing process and quality. Therefore, the first null hypothesis that there was no difference in influence of the three intaglio surface areas on the crown adaptation (fit), was rejected because the intaglio marginal area had a significantly higher influence on the crown adaptation than the intaglio axial and occlusal areas. Two outcomes emphasize this first hypothesis rejection. First, the intaglio axial area trueness was much better (lower RMS) than that of the intaglio marginal and occlusal areas for all the manufacturing processes tested (Table 1). This was not reflected in a better (uniform and thinner) cement-space thickness or higher percentage of a clinically accepted (<120-µm) cement-space thickness in the axial third (Fig. 2). Second and most importantly, the group with overall significantly better crown adaptation (Ini_HT) showed, solely in the intaglio marginal area, significant higher trueness values when compared to the other two groups.

Based on this marginal-area trueness - whole crown-adaptation correlation, the better the trueness, the closer the actual cement-space thickness must approximate the set spacer thickness. In this regard, the significantly better (lower) RMS and lower undercut (max) index at the Ini_HT intaglio marginal area (Table 1) explains the lower cement-space thickness not only at the marginal third but also at the axial third and all thirds combined (whole crown adaptation) (Table 2). Consequently, lower influence of the marginal area adaptation on the axial area was seen for this experimental group, with the mean cement-space thickness being 81 and 86 µm at the marginal and axial third, respectively (Table 2 and Fig. 2e), hereby additionally having resulted in a relatively uniform cement space (Fig. 3b-c). For XJet and Cerec_Zir, the mean cement-space thickness increased, respectively, from 94 µm in the marginal third to 106 µm in the axial third, and from 100 µm to 114 µm (Table 2 and Fig. 2e).

Although the better cement-space performance presented by Ini_HT can easily be explained by the overall better accuracy, explaining the difference in adaptation (fit) between XJet and Cerec_Zir is less evident. Significant difference in trueness between XJet and Cerec_Zir was found just in terms of overcut (min) at the intaglio occlusal area. However, even without significant difference with

Cerec_Zir, the XJet AM data, mainly in terms of undercut and RMS at the intaglio marginal area, are generally in between those recorded for the two milling SM experimental groups (Table 1; Fig. 2b-c). Regarding crown adaptation, in the marginal third the cement-space volume of XJet was statistically different from that recorded for both milling groups, while the cement-space thickness of XJet was statistically similar to that of Cerec_Zir and the clinically accepted (<120-µm) cement-space thickness of XJet was statistically similar to that of Ini_HT (Table 2; Fig. 2d-f). Overall, a relatively similar trueness and sometimes better crown-adaptation performance were recorded for Xjet as compared to Cerec_Zir. However, the worst results have been recorded for Xjet as compared to laboratory milling (Ini_HT). Hence, the second hypothesis that the geometric accuracy and subsequent adaptation of the 3D-printed FDPs were similar to those of chairside and laboratory milled ones, was accepted for XJet as compared to Cerec_Zir, but rejected for XJet as compared to Ini-HT. Similar results were found by Wang *et al.* (2019), who used stereolithography (SLA) as AM technique [39]. They concluded that zirconia crowns produced by SLA 3D-printing meet the trueness requirements for clinical use.

In this study, the intaglio axial area showed the best trueness, followed by the intaglio marginal and occlusal area (Table 1). Interestingly, the trueness recorded at all areas for AM (XJet) was in line with that measured for the two SM (milling) experimental groups, showing a similar pattern (Fig. 2). The first explanation for this pattern could be related to manufacturing influences since the axial-occlusal transition area at the intaglio inner surface seems most critical for both manufacturing methods. While SM (milling) is limited in reproducing this area due to the bur configuration(s) [13,22,45,46], AM is more error-prone at curved than vertical surfaces, hereby affecting trueness at large grooves and corner angles of crowns [39]. Besides milling/printing inaccuracy in this area, a second potential source of geometric inaccuracies could be due to shrinkage during zirconia sintering [17]. The sintering-shrinkage rate (SSR) is known to be non-uniform at different crown areas, while also the object shape and size influence the direction of the dimensional changes [11]. A smaller SSR is expected along the vertical (axial) axis when compared to a more horizontal plane, as the occlusal area [4,11]. Due to both these factors, the least optimum trueness and crown adaptation was

expected in the occlusal area/third for both SM and AM manufacturing processes and can be considered a risk factor for FDP fracture, since a thicker occlusal cement space was shown to lead to higher stress concentration [11,22,26]. Other research using two different SLA (AM) systems confirmed that the largest restoration-prep gap was found at the occlusal third [47]. Indeed, a significantly lower clinically acceptable (<120 μm) cement-space percentage of 46.7%, 36.3% and 25.1% was also measured at the occlusal third in this study for, respectively, Ini_HT, XJet and Cerec_Zir (Table 2). The lower percentage recorded for Cerec_Zir could additionally be justified by its significantly higher overcut (min) at the intaglio occlusal area (Table 1).

These dimensional changes induced by sintering shrinkage and manufacturing limitations, as well as the approximations embedded in the digital workflow [7,47], need to be corrected/adjusted [7,37]. Theoretically, contemporary CAD software can accurately compensate for them [6]. However, no manufacturing process is 100% accurate and will always involve some inherent input/output variation. These variations/irregularities, resulting from factors related to both the manufacturing device and the processed materials [17], should be within a production-tolerance range, this to avoid premature contacts and, ultimately, to provide the originally designed cement-space gap. In other words, although the cement-space thickness should be designed as thinly as possible, it should on the other hand be sufficiently thick to compensate for intaglio-surface irregularities [13,14,48], which at the same time should be within the engineering tolerance of CAD/CAM processing. Our results suggest that the marginal trueness of Ini_HT best met the CAM-tolerance limits, since the resultant cement-space thickness at the marginal and axial thirds most closely approached the set spacer thickness of 80 μm (Table 2). This uniformity resulted into the high clinically accepted (<120-μm) cement-space thickness for Ini-HT in the marginal third, which was maintained in the axial third (Figs. 2f and 3, and Table 2: 91.3% and 90.6%, respectively). XJet and Cerec_Zir however presented a decline in the clinically accepted (<120-μm) cement-space thickness from the marginal to the axial third (Table 2: from 88.9% to 72.8%, and from 79.0% to 63.8%, respectively). For XJet and Cerec_Zir, the higher RMS, undercut (max; e.g. precontact) and overcut (min; e.g. chipping) indices resulted in an increase of the cement-space volume/thickness and decrease of the clinically accepted (<120-μm)

cement-space thickness. Using CAD/CAM, Mously *et al.* (2014) detected no difference in marginal gap formation when the spacer thickness was set to 60 or 100 µm [14]. This could mean that these values were within the tolerance of the material/device combination used.

Engineering tolerance is not yet well developed for FDP manufacturing [37]. In dentistry, it has been explored more for dental implants [49] and tooth models [50]. Some studies that evaluated FDP adaptation used a 100-µm clinical acceptability as reference to evaluate crown adaptation, as was proposed for tooth models [47]. However, tolerance naturally differs depending on the application [37], and probably, taking into account the above-documented primary determining effect of the marginal area, differs also in between the intaglio regions. Such a tolerance concept should also be applied for the FDP's external surface, this to avoid having to re-shape the external FDP surface intraorally. Ideally, any intra-oral modification should no longer be needed when using modern/digital CAD/CAM workflows [6]. In this sense, the study results revealed that the external crown accuracy achieved by XJet was in line with that of the chairside and laboratory milling devices.

In this study, all three experimental groups showed a clinically acceptable mean cement-space thickness in the marginal third (Table 2: 81 µm for Ini-HT; 94 µm for Xjet; 100 µm for Cerec_Zir). Even though a direct comparison of these mean cement-space thickness data with literature data is possible, conclusions based on mean cement-space thickness (marginal gap) do not provide adequate/sufficient information to assess clinical acceptability of crown adaptation (fit) [19,24]. Doing this would mask flaws and limit knowledge, as compared to the information non-destructive cement-space characterization in 3D using micro-CT can provide. Using micro-CT, this study enabled to assess crown adaptation in 3D, providing more clinically relevant data. Micro-CT enabled full characterization of the cement-space volume that additionally was further subdivided into thickness intervals (cement-space thickness distribution), by which clinically acceptable (<120 µm) crown adaptation could be presented in percentages (Table 2 and Fig. 3) [25]. For example, although the mean cement-space thickness for the whole crown adaptation of Cerec_Zir was 124 µm (Table 2: 102 µm for Ini-HT; 113 µm for Xjet), solely 54.6% of the cement-space volume met the clinically acceptable 120-µm norm (Table 2: 73.1% for Ini-HT; 64.9% for Xjet) [44]. This percentage increased

to 79.0% for Cerec_Zir when considering only the marginal third. From an opposite perspective, even with a not that much lower mean cement-space thickness of 102 µm recorded for Ini_HT, as much as 73.1% of the cement-space thickness recorded for Ini_HT met the clinically acceptable 120-µm norm. These results are in line with Matta *et al*. (2012), who reported that 75% of the measured cement-space thickness recorded for zirconia single crown copings met the clinically acceptable 120-µm norm [19]. The in-this-study employed cement-space thickness-distribution analysis is more sensitive and provides detailed and more clinically relevant information beyond reporting solely mean cement-space thickness performance. It enables assessment of cement-space uniformity and, when subdivided into thirds, allows an in-depth study of the crown-adaptation (mis)fit quality, which may vary significantly among different crown regions.

Furthermore, the discriminative power of the cement-space thickness-distribution analysis allows detecting specific flaws that compromise crown adaptation. An interesting example of how support material influenced crown adaptation in this study can be seen in Fig. 4a-c. The attached 3D-printed agglomerate at the axial area was 151 µm high and led to an increased axial cement-space volume of 5.20 mm^3, being substantially higher than the mean axial cement-space volume of 4.57 mm^3 that was recorded for Xjet. The clinically acceptable (<120 µm) crown adaptation dropped from 72.8% (mean <120-µm percentage mentioned in Table 2) to 65% at the axial third for the crown in Fig. 5. Although the 'whole crown adaptation' cement-space volume of this crown was larger (9.75 mm^3) compared to the mean (Table 2: 9.32 mm^3), the cement-space volume was smaller in the marginal third (1.84 mm^3 for this crown compared to the mean volume of 2.05 mm^3) and similar in the occlusal third (2.71 mm^3 for this crown compared to the mean volume of 2.69 mm^3). Surprisingly, the smaller marginal third cement-space volume presented a lower clinically acceptable (<120 µm) 'whole crown adaptation' percentage of 58% as compared to the mean (64.9%).

SM and AM manufacturing accuracy is accomplished by virtually slicing the CAD model in parallel planes perpendicular to, respectively, the milling and printing direction. AM characteristically results in a layered surface texture (Fig. 5c), by which AM manufacturing accuracy highly depends on the print direction and the printed layer thickness, as well as on the amount of support material, if

employed [4]. In analogy to AM, SM involves a bur-cutting direction, resulting in milling lines corresponding to the distance between two parallel planes in the CAM model. The width of the milling lines, the bur tip geometry and the axis number of the milling unit will directly affect the milling accuracy (Fig. 5a-b) [7]. As documented before [2,6,14], a chairside 4-axis milling unit resulted in less favorable crown adaptation (fit) when compared to restorations that were milled using a laboratory 5-axis milling unit, this because of the higher trueness of the latter laboratory milling unit. In this study, comparing two milling devices, Ini_HT achieved significantly better (lower) RMS and undercut (max) indices in the intaglio marginal area than Cerec_Zir (Table 1). Part of these findings should also be explained by flaws commonly introduced by the weaker mechanical structure (robustness) of the chairside milling unit, inducing vibrations and shocks during milling, of which the results can be seen in Fig. 4d-f [7]. Since chairside milling units weigh much less and consequently are less stable/robust, the introduced micro-cracks will directly affect the restoration geometry and strength, with failure during clinical functioning more likely expected to occur earlier [4,7]. This, combined with ceramics' brittle nature, frequently causes edge chipping at the thin restoration margins and possibly even radial cracks, which may severely affect the marginal adaptation of the restoration to the tooth preparation and ultimately reduce the restoration's clinical lifetime.

Although the study results revealed that XJet 3D-printing achieved an accuracy similar to that of the milling devices evaluated, further investigation of the mechanical properties of XJet FDPs along with clinical research is needed to determine whether this 3D-printing technology is ready for use in clinical practice. In addition, the zirconia-shrinkage process of complex-shaped objects (restorations) as well as the FDP-manufacturing tolerance should be better understood to further improve accurate manufacturing predictability and consistency. A possible limitation of the present study concerns the different post-processing procedures involved in the three manufacturing processes, such as there were differences in green body handling, sintering and AM debinding. Another limitation could have been the authors' choice to have used wax to hold the crown in position on the tooth prep, which may have influenced perfect crown adaptation/seating. This wax fixation was however very carefully executed, as detailed in the Materials and Methods. In addition, the cement-space thickness-

distribution analysis and virtual qualitative evaluation by micro-CT confirmed accurate seating since the outlier results could be attributed to manufacturing flaws, as they were explored further in Fig. 4.

CONCLUSIONS

3D-printed monolithic zirconia crowns presented trueness and crown-adaptation performance in line with that recorded for chairside milling following the procedures investigated in this study. The inkjet 3D-printing process used in this study can be considered to have provided sufficient manufacturing accuracy for clinical use. Laboratory milling showed better performance in the intaglio's marginal area, which appeared most determining for the differences recorded between the three manufacturing processes. Therefore, accurate milling and printing of the intaglio's marginal area is primordial and should be prioritized when manufacturing FDPs. The more complete tri-dimensional analysis of the trueness influence on the cement-space characteristics, as revealed by combining visible-light scanning and micro-CT, helped to better understand the manufacturing limitations of both the restorative materials and manufacturing devices. Regarding monolithic zirconia crowns, the least optimum trueness and crown adaptation can be expected at the intaglio's occlusal area for both SM and AM manufacturing processes.

References

[1] Bousnaki M, Chatziparaskeva M, Bakopoulou A, Pissiotis A, Koidis P. Variables affecting the fit of zirconia fixed partial dentures: A systematic review. J Prosthet Dent 2020;123:686-692.e8. https://doi.org/10.1016/j.prosdent.2019.06.019.

[2] Kirsch C, Ender A, Attin T, Mehl A. Trueness of four different milling procedures used in dental CAD/CAM systems. Clin Oral Investig 2017;21:551–8. https://doi.org/10.1007/s00784-016-1916-y.

[3] Moldovan O, Luthardt RG, Corcodel N, Rudolph H. Three-dimensional fit of CAD/CAM-made zirconia copings. Dent Mater 2011;27:1273–8. https://doi.org/10.1016/j.dental.2011.09.006.

[4] Revilla-León M, Methani MM, Morton D, Zandinejad A. Internal and marginal discrepancies associated with stereolithography (SLA) additively manufactured zirconia crowns. J Prosthet Dent 2020;124:730–7. https://doi.org/10.1016/j.prosdent.2019.09.018.

[5] Sailer I, Makarov NA, Thoma DS, Zwahlen M, Pjetursson BE. All-ceramic or metal-ceramic tooth-supported fixed dental prostheses (FDPs)? A systematic review of the survival and complication rates. Part I: Single crowns (SCs). Dent Mater 2015;31:603–23. https://doi.org/10.1016/j.dental.2015.02.011.

[6] Bosch G, Ender A, Mehl A. A 3-dimensional accuracy analysis of chairside CAD/CAM milling processes. J Prosthet Dent 2014;112:1425–31. https://doi.org/10.1016/j.prosdent.2014.05.012.

[7] Tapie L, Lebon N, Mawussi B, Duret F. Understanding dental CAD / CAM for restorations – accuracy from a mechanical engineering viewpoint Comprendre la CFAO pour les restaurations dentaire – la précision vue de l ' ingénierie mécanique. Int J Comput Dent 2015;18:343–67.

[8] Piconi C, Maccauro G. Zirconia as a ceramic biomaterial. Biomaterials 1999;20:1–25. https://doi.org/10.1016/S0142-9612(98)00010-6.

[9] Zhang Y, Lawn BR. Novel Zirconia Materials in Dentistry. J Dent Res 2018;97:140–7. https://doi.org/10.1177/0022034517737483.

[10] Ban S. Classification and Properties of Dental Zirconia as Implant Fixtures and Superstructures. Materials (Basel) 2021;14. https://doi.org/https://doi.org/10.3390/ma14174879.

[11] Edwards Rezende CE, Sanches Borges AF, Macedo RM, Rubo JH, Griggs JA. Dimensional changes from the sintering process and fit of Y-TZP copings: Micro-CT analysis. Dent Mater 2017;33:e405–13. https://doi.org/10.1016/j.dental.2017.08.191.

[12] Hamza TA, Sherif RM. In vitro evaluation of marginal discrepancy of monolithic zirconia restorations fabricated with different CAD-CAM systems. J Prosthet Dent 2017;117:762–6. https://doi.org/10.1016/j.prosdent.2016.09.011.

[13] Sailer I, Benic GI, Fehmer V, Hämmerle CHF, Mühlemann S. Randomized controlled within-subject evaluation of digital and conventional workflows for the fabrication of lithium disilicate single crowns. Part II: CAD-CAM versus conventional laboratory procedures. J Prosthet Dent 2017;118:43–8. https://doi.org/10.1016/j.prosdent.2016.09.031.

[14] Mously HA, Finkelman M, Zandparsa R, Hirayama H. Marginal and internal adaptation of ceramic crown restorations fabricated with CAD/CAM technology and the heat-press technique. J Prosthet Dent 2014;112:249–56. https://doi.org/10.1016/j.prosdent.2014.03.017.

[15] Schriwer C, Skjold A, Gjerdet NR, Øilo M. Monolithic zirconia dental crowns. Internal fit, margin quality, fracture mode and load at fracture. Dent Mater 2017;33:1012–20. https://doi.org/10.1016/j.dental.2017.06.009.

[16] Denry I. How and when does fabrication damage adversely affect the clinical performance of ceramic restorations? Dent Mater 2013;29:85–96. https://doi.org/10.1016/j.dental.2012.07.001.

[17] Papadiochou S, Pissiotis AL. Marginal adaptation and CAD-CAM technology: A systematic review of restorative material and fabrication techniques. J Prosthet Dent 2018;119:545–51. https://doi.org/10.1016/j.prosdent.2017.07.001.

[18] Rungruanganunt P, Kelly JR, Adams DJ. Two imaging techniques for 3D quantification of pre-cementation space for CAD/CAM crowns. J Dent 2010;38:995–1000.

https://doi.org/10.1016/j.jdent.2010.08.015.

[19] Matta RE, Schmitt J, Wichmann M, Holst S. Circumferential fit assessment of CAD/CAM single crowns--a pilot investigation on a new virtual analytical protocol. Quintessence Int 2012;43:801–9.

[20] Groten M, Axmann D, Pröbster L, Weber H. Determination of the minimum number of marginal gap measurements required for practical in vitro testing. J Prosthet Dent 2000;83:40–9. https://doi.org/10.1016/S0022-3913(00)70087-4.

[21] Holmes JR, Bayne SC, Holland GA, Sulik WD. Considerations in measurement of marginal fit 1984:405–8.

[22] Mahmood DJH, Braian M, Larsson C, Wennerberg A. Production tolerance of conventional and digital workflow in the manufacturing of glass ceramic crowns. Dent Mater 2019;35:486–94. https://doi.org/10.1016/j.dental.2019.01.015.

[23] Balkaya MC, Cinar A, Pamuk S. Influence of firing cycles on the margin distortion of 3 all-ceramic crown systems. J Prosthet Dent 2005;93:346–55. https://doi.org/10.1016/j.prosdent.2005.02.003.

[24] Gonzalo E, Suárez MJ, Serrano B, Lozano JFL. A comparison of the marginal vertical discrepancies of zirconium and metal ceramic posterior fixed dental prostheses before and after cementation. J Prosthet Dent 2009;102:378–84. https://doi.org/10.1016/S0022-3913(09)60198-0.

[25] Santos TMP, Ferreira CG, Araújo OMO, Machado AS, Silva ASS, Lopes RT. Methodology to analyze the marginal fit of odontological crowns through tridimensional parameters using X-ray microCT technique. Radiat Phys Chem 2020;167. https://doi.org/10.1016/j.radphyschem.2019.04.040.

[26] Rezende CEE, Borges AFS, Gonzaga CC, Duan Y, Rubo JH, Griggs JA. Effect of cement space on stress distribution in Y-TZP based crowns. Dent Mater 2017;33:144–51. https://doi.org/10.1016/j.dental.2016.11.006.

[27] Pelekanos S, Koumanou M, Koutayas SO, Zinelis S, Eliades G. Micro-CT evaluation of the

marginal fit of different In-Ceram alumina copings. Eur J Esthet Dent 2009;4:278–92.

[28] Souza ROA, Özcan M, Pavanelli CA, Buso L, Lombardo GHL, Michida SMA, et al. Marginal and Internal Discrepancies Related to Margin Design of Ceramic Crowns Fabricated by a CAD/CAM System. J Prosthodont 2012;21:94–100. https://doi.org/10.1111/j.1532-849X.2011.00793.x.

[29] De Jager N, Pallav P, Feilzer AJ. The influence of design parameters on the FEA-determined stress distribution in CAD-CAM produced all-ceramic dental crowns. Dent Mater 2005;21:242–51. https://doi.org/10.1016/j.dental.2004.03.013.

[30] De Jager N, Pallav P, Feilzer AJ. The apparent increase of the Young's modulus in thin cement layers. Dent Mater 2004;20:457–62. https://doi.org/10.1016/j.dental.2003.07.002.

[31] Kohorst P, Junghanns J, Dittmer MP, Borchers L, Stiesch M. Different CAD/CAM-processing routes for zirconia restorations: influence on fitting accuracy. Clin Oral Investig 2011;15:527–36. https://doi.org/10.1007/s00784-010-0415-9.

[32] Marker VA, Miller AW, Miller BH, Swepston JH. Factors affecting the retention and fit of gold castings. J Prosthet Dent 1987;57:425–30. https://doi.org/10.1016/0022-3913(87)90007-2.

[33] Wang W, Sun J. Dimensional accuracy and clinical adaptation of ceramic crowns fabricated with the stereolithography technique. J Prosthet Dent 2020. https://doi.org/10.1016/j.prosdent.2020.02.032.

[34] Ebert J, Özkol E, Zeichner A, Uibel K, Weiss Ö, Koops U, et al. Direct inkjet printing of dental prostheses made of zirconia. J Dent Res 2009;88:673–6. https://doi.org/10.1177/0022034509339988.

[35] Özkol E, Zhang W, Ebert J, Telle R. Potentials of the " Direct inkjet printing" method for manufacturing 3Y-TZP based dental restorations. J Eur Ceram Soc 2012;32:2193–201. https://doi.org/10.1016/j.jeurceramsoc.2012.03.006.

[36] Willems E, Turon-Vinas M, Camargo dos Santos B, Van Hooreweder B, Zhang F, Van Meerbeek B, et al. Additive manufacturing of zirconia ceramics by material jetting. J Eur Ceram Soc 2021;41:5292–306. https://doi.org/10.1016/j.jeurceramsoc.2021.04.018.

[37] Braian M, Jimbo R, Wennerberg A. Production tolerance of additive manufactured polymeric

objects for clinical applications. Dent Mater 2016;32:853–61. https://doi.org/10.1016/j.dental.2016.03.020.

[38] Tapie L, Lebon N, Mawussi B, Duret F. Understanding dental CAD / CAM for restorations – accuracy from a mechanical engineering viewpoint Comprendre la CFAO pour les restaurations dentaire – la précision vue de l ' ingénierie mécanique. Int J Comput Dent 2015;18:343–67.

[39] Wang W, Yu H, Liu Y, Jiang X, Gao B. Trueness analysis of zirconia crowns fabricated with 3-dimensional printing. J Prosthet Dent 2019;121:285–91. https://doi.org/10.1016/j.prosdent.2018.04.012.

[40] Osman RB, van der Veen AJ, Huiberts D, Wismeijer D, Alharbi N. 3D-printing zirconia implants; a dream or a reality? An in-vitro study evaluating the dimensional accuracy, surface topography and mechanical properties of printed zirconia implant and discs. J Mech Behav Biomed Mater 2017;75:521–8. https://doi.org/10.1016/j.jmbbm.2017.08.018.

[41] Beschnidt SM, Strub JR. Evaluation of the marginal accuracy of different all-ceramic crown systems after simulation in the artificial mouth. J Oral Rehabil 1999;26:582–93. https://doi.org/10.1046/j.1365-2842.1999.00449.x.

[42] Okutan M, Heydecke G, Butz F, Strub JR. Fracture load and marginal fit of shrinkage-free ZrSiO4 all-ceramic crowns after chewing simulation. J Oral Rehabil 2006;33:827–32. https://doi.org/10.1111/j.1365-2842.2006.01637.x.

[43] Hildebrand T, Rüegsegger P. A new method for the model-independent assessment of thickness in three-dimensional images. J Microsc 1997;185:67–75. https://doi.org/10.1046/j.1365-2818.1997.1340694.x.

[44] McLean JW, Von F. The estimation of cement film thickness by an in vivo technique. Br Dent J 1971;131:107–11. https://doi.org/10.1038/sj.bdj.4802708.

[45] Örtorp A, Jönsson D, Mouhsen A, Vult Von Steyern P. The fit of cobalt-chromium three-unit fixed dental prostheses fabricated with four different techniques: A comparative in vitro study. Dent Mater 2011;27:356–63. https://doi.org/10.1016/j.dental.2010.11.015.

[46] Borba M, Cesar PF, Griggs JA, Della Bona Á. Adaptation of all-ceramic fixed partial dentures. Dent Mater 2011;27:1119–26. https://doi.org/10.1016/j.dental.2011.08.004.

[47] Wang W, Sun J. Dimensional accuracy and clinical adaptation of ceramic crowns fabricated with the stereolithography technique. J Prosthet Dent 2021;125:657–63. https://doi.org/10.1016/j.prosdent.2020.02.032.

[48] Grajower R, Zuberi Y, Lewinstein I. Improving the fit of crowns with die spacers. J Prosthet Dent 1989;61:555–63. https://doi.org/10.1016/0022-3913(89)90275-8.

[49] Braian M, Bruyn H, Fransson H, Christersson C, Wennerberg A. Tolerance Measurements on Internal- and External-Hexagon Implants. Int J Oral Maxillofac Implants 2014;29:846–52. https://doi.org/10.11607/jomi.3242.

[50] Rungrojwittayakul O, Kan JY, Shiozaki K, Swamidass RS, Goodacre BJ, Goodacre CJ, et al. Accuracy of 3D Printed Models Created by Two Technologies of Printers with Different Designs of Model Base. J Prosthodont 2020;29:124–8. https://doi.org/10.1111/jopr.13107.

TABLES

Table 1 - Trueness (µm) in terms of overcut (min), undercut (max) and trueness deviation (RMS) for the three intaglio's surface areas and the external surface.

Areas	Intaglio marginal area			Intaglio axial area			Intaglio occlusal area			External surface area		
	Overcut (min)	Undercut (max)	Trueness dev. (RMS)	Overcut (min)	Undercut (max)	Trueness dev. (RMS)	Overcut (min)	Undercut (max)	Trueness dev. (RMS)	Overcut (min)	Undercut (max)	Trueness dev. (RMS)
Cerec_Zir	-560±6[a]	385±5[a]	100±17[a]	-210±162[a]	296±172[a]	39±16[a]	-291±103[a]	690±145[a]	121±38[a]	-977±253[a]	806±231[a]	81±28[a]
Ini_HT	-434±11[a]	200±11[b]	75±19[b]	-269±87[a]	258±68[a]	37±13[a]	-190±87[b]	733±277[a]	123±54[a]	-830±155[a]	791±303[a]	75±18[a]
Xjet	-567±19[a]	334±8[a]	97±20[a]	-221±52[a]	286±100[a]	33±7[a]	-154±139[b]	701±184[a]	127±54[a]	-754±181[a]	622±177[a]	64±12[a]

Different supercript letters indicate statistically significant differences ($p<0.05$).

Table 2 - Crown adaptation in terms of cement-space volume, thickness and percentage below 120-µm thickness for the whole crown adaptation and the three thirds.

Region	Whole crown adaptation			Marginal third			Axial third			Occlusal third		
	Volume ($x10^{12}$ µm³)	Thickness (µm)	Percentage < 120 µm	Volume ($x10^{12}$ µm³)	Thickness (µm)	Percentage < 120 µm	Volume ($x10^{12}$ µm³)	Thickness (µm)	Percentage < 120 µm	Volume ($x10^{12}$ µm³)	Thickness (µm)	Percentage < 120 µm
Cerec_Zir	9.67[a]	124[a]	54.6%[a]	2.29[a]	100[a]	79.0%[a]	4.36[a]	114[a]	63.8%[a]	2.98[a]	154[a]	25.1%[a]
Ini_HT	7.98[b]	102[b]	73.1%[b]	1.65[b]	81[b]	91.3%[b]	3.62[b]	86[b]	90.6%[b]	2.58[a]	127[b]	46.7%[b]
Xjet	9.32[a]	113[a]	64.9%[b]	2.05[c]	94[a]	88.9%[b]	4.57[a]	106[a]	72.8%[a]	2.69[a]	135[b]	36.3%[ab]

Different supercript letters indicate statistically significant differences ($p<0.05$).

Table 3 - Spearman correlation between trueness and cement-space characteristics.										
Trueness		**Intaglio marginal area**			**Intaglio axial area**			**Intaglio occlusal area**		
Crown adaptation		Overcut (min)	Undercut (max)	Trueness dev. (RMS)	Overcut (min)	Undercut (max)	Trueness dev. (RMS)	Overcut (min)	Undercut (max)	Trueness dev. (RMS)
Whole crown adaptation	Volume (mm)	**-0.414**$^{(B)}$	**0.416**$^{(B)}$	**0.575**$^{(A)}$	0.269	0.134	0.024	-0.134	-0.115	-0.073
	Thickness (µm)	-0.361	**0.398**$^{(B)}$	**0.519**$^{(A)}$	0.268	0.204	0.051	-0.229	-0.121	-0.079
	Percentage (<120 µm)	**-0.384**$^{(B)}$	**-0.369**$^{(B)}$	**-0.501**$^{(A)}$	-0.285	-0.197	-0.032	0.302	0.142	0.092
Marginal third	Volume (mm)	-0.219	**0.522**$^{(A)}$	**0.443**$^{(B)}$	0.301	0.079	0.012	-0.362	-0.023	-0.018
	Thickness (µm)	-0.282	**0.498**$^{(A)}$	**0.518**$^{(A)}$	**0.399**$^{(B)}$	0.120	-0.060	-0.265	-0.210	-0.201
	Percentage (<120 µm)	-0.028	-0.190	-0.216	-0.267	-0.027	-0.020	0.336	0.252	0.254
Axial third	Volume (mm)	**-0.445**$^{(B)}$	0.354	**0.547**$^{(A)}$	0.300	0.084	-0.091	-0.025	-0.064	-0.015
	Thickness (µm)	**-0.476**$^{(A)}$	**0.460**$^{(B)}$	**0.597**$^{(A)}$	0.355	0.135	-0.097	-0.228	-0.021	0.034
	Percentage (<120 µm)	**0.480**$^{(A)}$	**-0.507**$^{(A)}$	**-0.599**$^{(A)}$	-0.366	-0.196	0.073	0.276	-0.010	-0.069
Occlusal third	Volume (mm)	-0.049	0.016	0.213	0.025	0.144	0.228	-0.155	-0.144	-0.109
	Thickness (µm)	-0.087	0.089	0.249	-0.020	0.225	0.226	-0.259	-0.005	0.021
	Percentage (<120 µm)	0.215	-0.120	-0.312	-0.002	-0.271	-0.214	0.273	0.014	-0.036

(A) Correlation is significant at the 0.01 level (2-tailed); (B) Correlation is significant at the 0.05 level (2-tailed).

Figure legends

Fig. 1 Schematic illustrating the different evaluation methodologies (four rounded squares) and the two study parameters TRUENESS, as determined in terms of the overcut (min), undercut (max) and trueness deviation (RMS) indices at the intaglio occlusal, axial and marginal areas, and the external surface area, and CEMENT-SPACE CHARACTERISTICS, as determined in terms of cement-space volume, thickness and thickness distribution at the occlusal, axial and marginal thirds in (a) and (b), with a color map representing trueness deviation in (c), a micro-CT cross-section in (d) and a 3D color map of cement-space thickness distribution in (e).

Fig. 2 TRUENESS graphically presented in box plots (in mm) in terms of overcut (min) in (a), undercut (max) in (b), and trueness deviation (RMS) in (c), for the intaglio marginal, axial and occlusal areas, and CEMENT-SPACE CHARACTERTISTICS graphically presented in terms of cement-space volume (in mm^3) in (d), cement-space thickness (in µm) in (e), and in clinically acceptable cement-space thickness (<120 µm) percentage in (e).

Fig. 3 Cement-space thickness distribution graphically presented for the whole cement space (all thirds combined) in (a), the marginal third in (b), the axial third in (c), and the occlusal third in (d). As the cement layer should be as uniform and thin as possible [14], the resulting curve peak should be as low as possible and shifted to the left as much as possible. The grey square represents the cement-space volume distributed by cement-space thickness with a cement space below 120 µm considered as 'clinically acceptable' [44].

Fig. 4 An agglomerate of the XJet support material was attached to one axial wall, as imaged by SEM in (a), as shown in the crown-trueness reconstruction in (b), and as visualized in cross-section by micro-CT in (c). The agglomeration height was 151 µm, leading to a cement-space volume of 5.20 mm^3, while the mean cement-space volume was 4.57 mm^3 in the axial third, and to a cement-space volume of 9.75 mm^3 for all thirds combined as compared to the mean cement-space volume of 9.32

mm^3. The clinically acceptable (<120 µm) crown adaptation decreased from 65% to 58% for all thirds combined and from 73% to 65% in the axial third. A manufacturing defect or marginal chipping was detected in the marginal area of one Cerec_Zir specimen, as imaged by SEM in (d), as shown in the crown-trueness reconstruction in (e), as shown by overlapping the original CAD with the scanned manufactured crown in (f), and as visualized in the 3D model by micro-CT (g). Color maps were generated to represent trueness deviations in (e), revealing that the chipping depth was 200 µm. The marginal cement-space volume of this specific Cerec_Zir crown was higher (1.96 mm^3) than the mean cement-space volume of the experimental Cerec_Zir group (1.65 mm^3).

Fig. 5 Visible light-scanning images representing all three experimental groups, with the discretization steps and sweeping pattern of the chairside 4-axis and laboratory 5-axis milling devices shown in (a) and (b), respectively, while a surface-stepping phenomenon, being a 3D-printing characteristic superficial texture, was not clearly seen in (c), this probably caused by sintering. The white squares show the abovementioned specific structural features in a buccal-lingual incidence.

Fig. 1

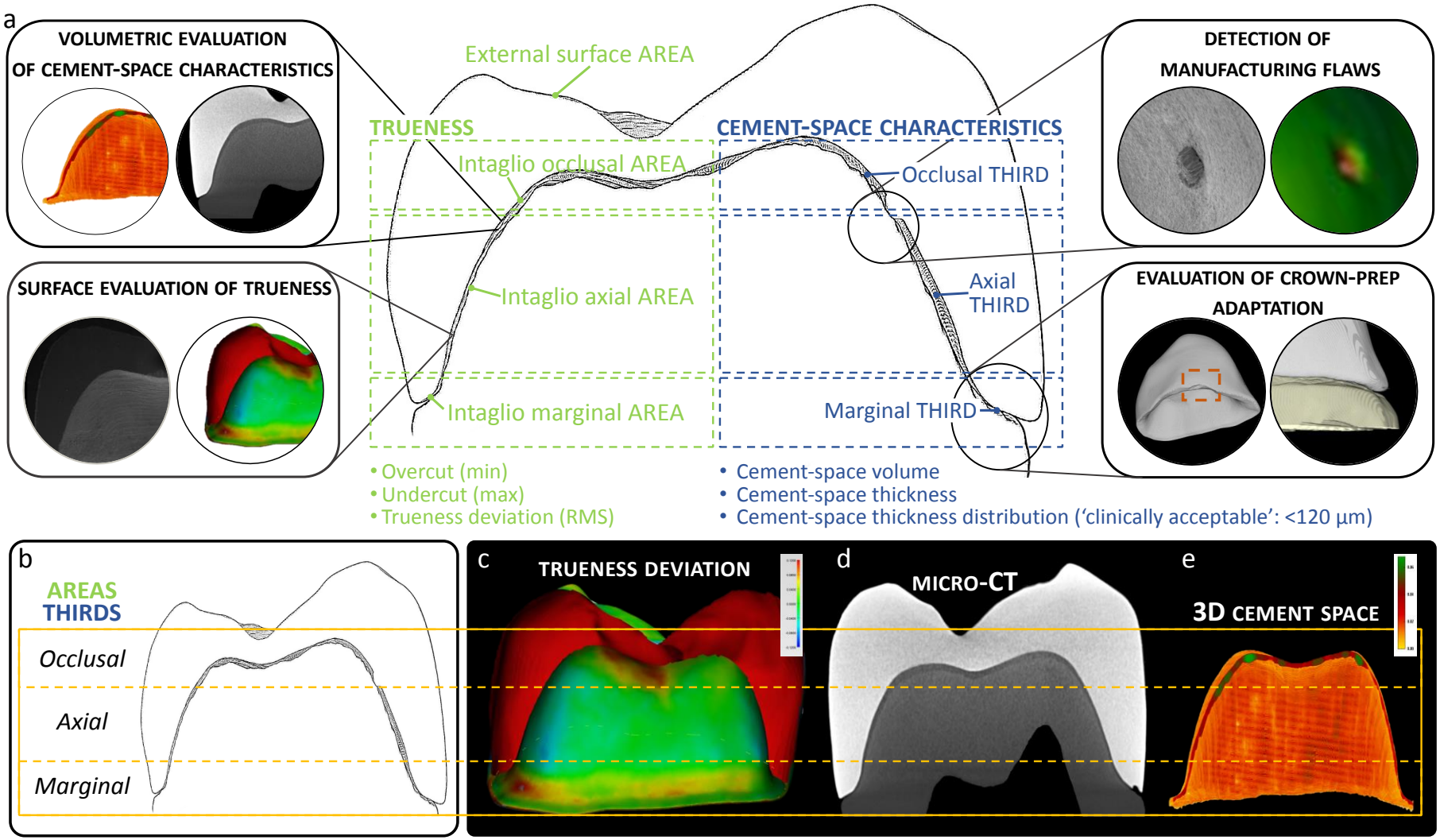
a
VOLUMETRIC EVALUATION
OF CEMENT-SPACE CHARACTERISTICS
SURFACE EVALUATION OF TRUENESS
External surface AREA
TRUENESS
Intaglio occlusal AREA
Intaglio axial AREA
Intaglio marginal AREA
CEMENT-SPACE CHARACTERISTICS
Occlusal THIRD
Axial THIRD
Marginal THIRD
DETECTION OF
MANUFACTURING FLAWS
EVALUATION OF CROWN-PREP
ADAPTATION
• Overcut (min)
• Undercut (max)
• Trueness deviation (RMS)
• Cement-space volume
• Cement-space thickness
• Cement-space thickness distribution ('clinically acceptable': <120 µm)
b
AREAS
THIRDS
Occlusal
Axial
Marginal
c
TRUENESS DEVIATION
d
MICRO-CT
e
3D CEMENT SPACE

Fig. 2

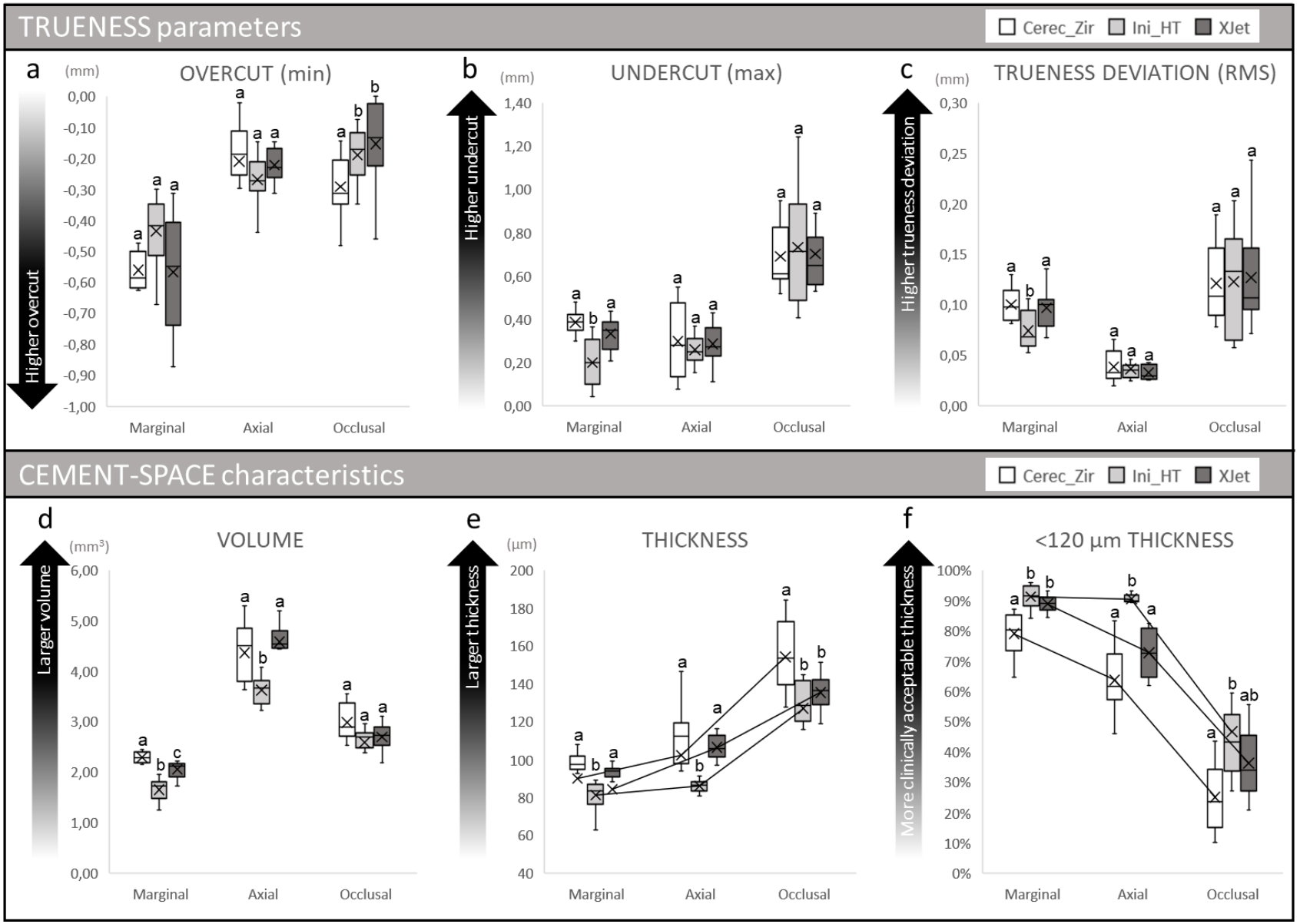
TRUENESS parameters
Cerec_Zir
Ini_HT
XJet
a
OVERCUT (min)
(mm)
Higher overcut
Marginal
Axial
Occlusal
b
UNDERCUT (max)
Higher undercut
c
TRUENESS DEVIATION (RMS)
Higher trueness deviation
CEMENT-SPACE characteristics
d
VOLUME
(mm³)
Larger volume
e
THICKNESS
(µm)
Larger thickness
f
<120 µm THICKNESS
More clinically acceptable thickness

Fig. 3

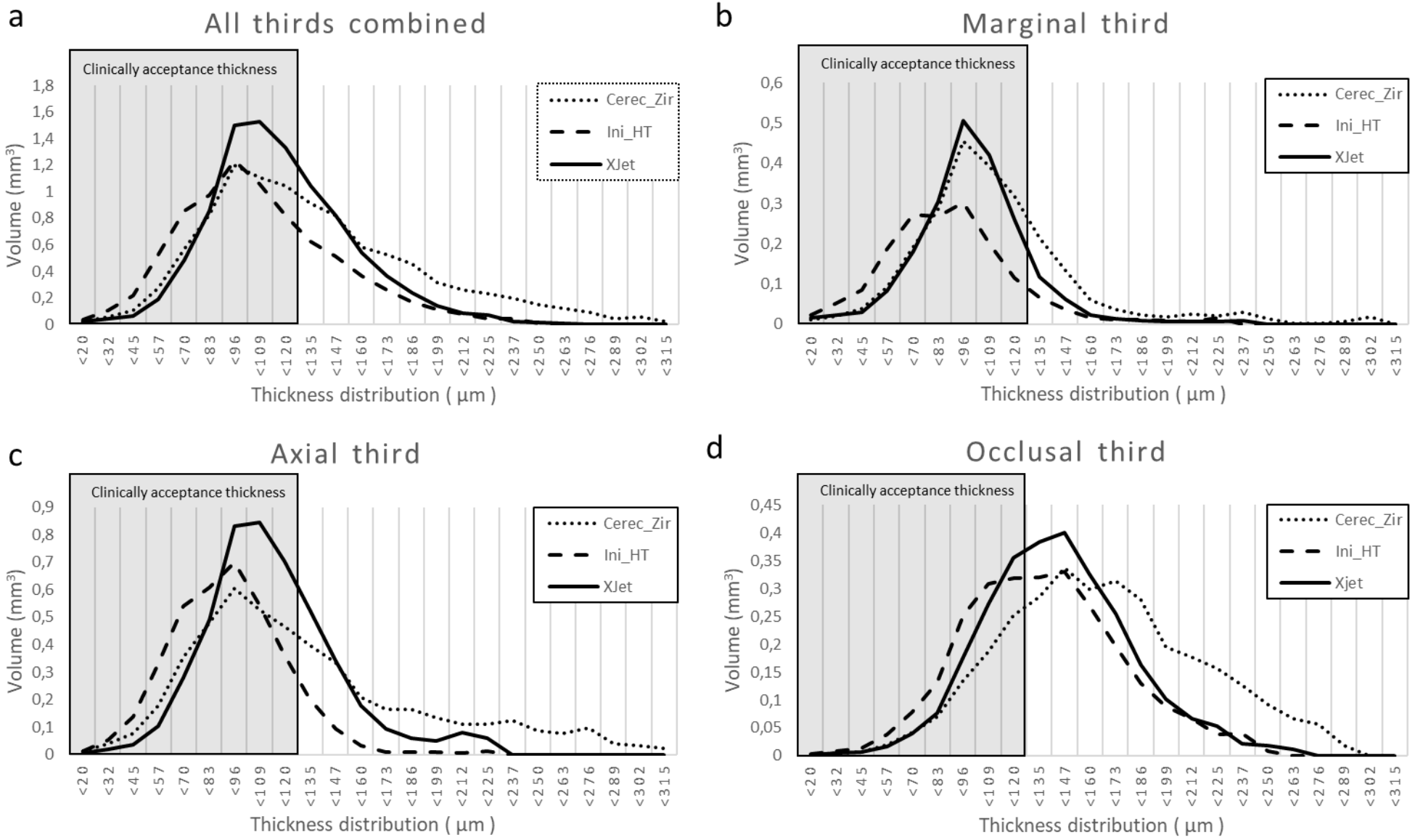
a
All thirds combined
Clinically acceptance thickness
Volume (mm³)
Thickness distribution (µm)
Cerec_Zir
Ini_HT
XJet
b
Marginal third
Clinically acceptance thickness
Volume (mm³)
Thickness distribution (µm)
Cerec_Zir
Ini_HT
XJet
c
Axial third
Clinically acceptance thickness
Volume (mm³)
Thickness distribution (µm)
Cerec_Zir
Ini_HT
XJet
d
Occlusal third
Clinically acceptance thickness
Volume (mm³)
Thickness distribution (µm)
Cerec_Zir
Ini_HT
Xjet

Fig. 4

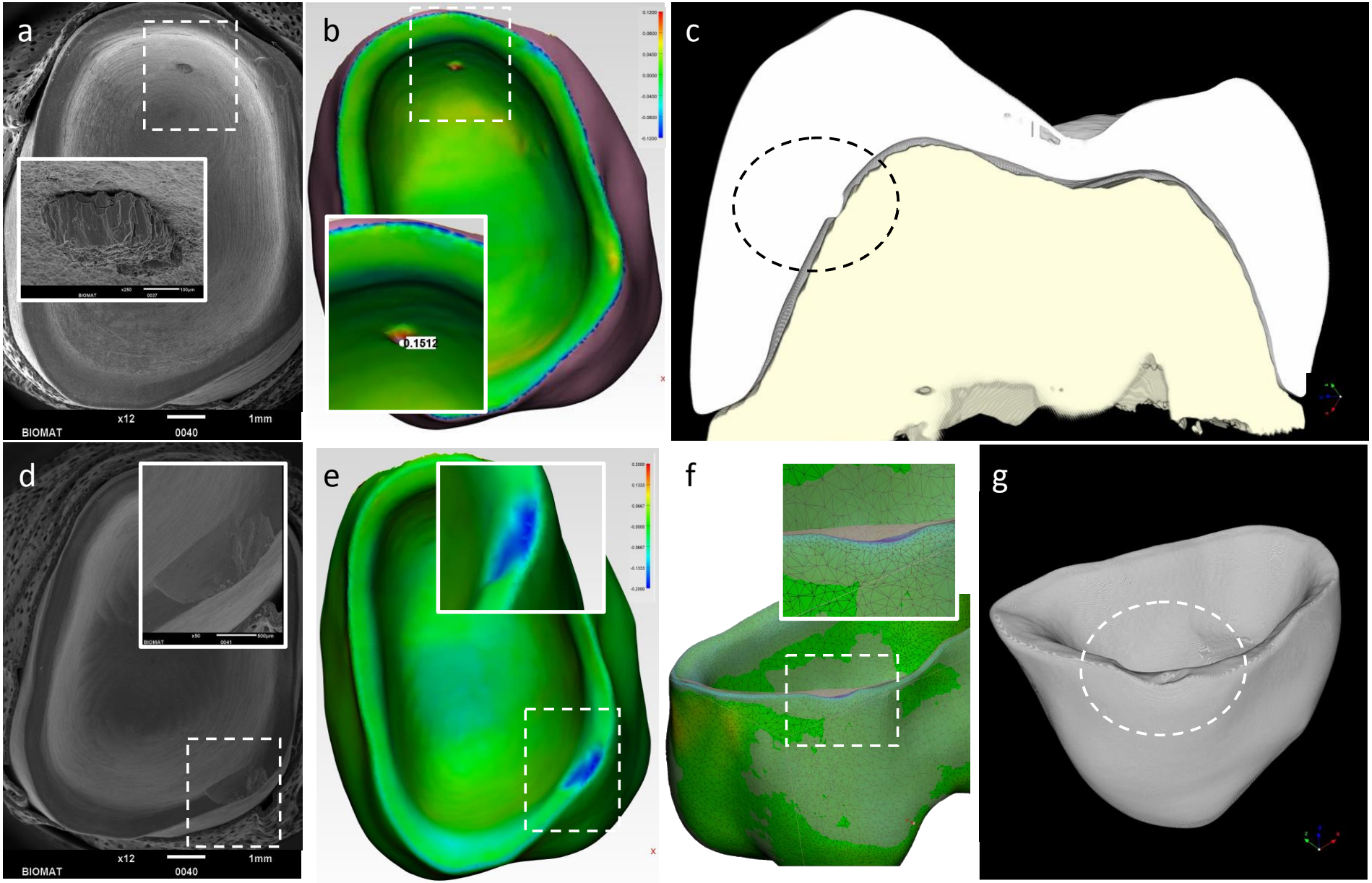

Fig. 5

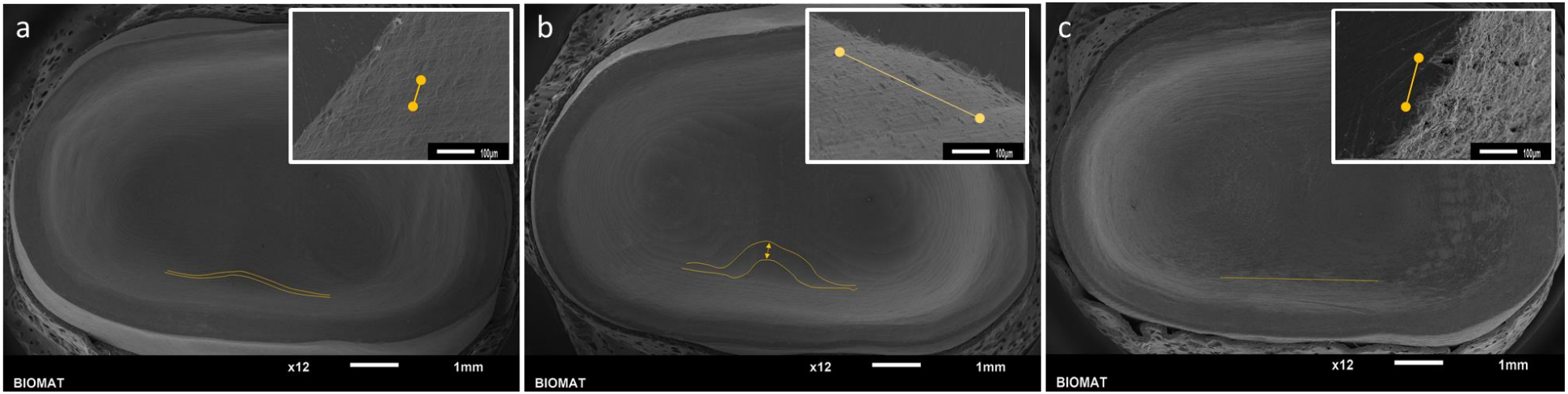
a
100µm
x12
1mm
BIOMAT
b
100µm
x12
1mm
BIOMAT
c
100µm
x12
1mm
BIOMAT